CHINESE OPTICS LETTERS

Vol. 20, No. 8 | August 2022

High-power narrow-linewidth diode laser pump source based on high-efficiency external cavity feedback technology

Jinliang Han (韩金樑)[1,2], Jun Zhang (张 俊)[1*], Xiaonan Shan (单肖楠)[1], Hangyu Peng (彭航宇)[1], Yawei Zhang (张亚维)[1], and Lijun Wang (王立军)[1]

[1] Changchun Institute of Optics, Fine Mechanics and Physics, Chinese Academy of Sciences, Changchun 130033, China

[2] University of Chinese Academy of Sciences, Beijing 100049, China

*Corresponding author: zhangjciomp@163.com

Received February 25, 2022 | Accepted April 28, 2022 | Posted Online May 25, 2022

In this research, the highly efficient external cavity feedback technology based on volume Bragg grating (VBG) is studied. By using the structure of a fast axis collimating lens, the beam transformation system, a slow axis collimating lens, and VBG, the divergence angle of the fast and slow axes of the diode laser incident on the VBG is reduced effectively, and the feedback efficiency of the external cavity is improved. Combined with beam combining technology, fiber coupling technology, and precision temperature control technology, a high-power and narrow-linewidth diode laser pump source of kilowatt class is realized for alkali metal vapor laser pumping. The core diameter of the optical fiber is 1000 μm, the numerical aperture is 0.22, the output power from the fiber is 1013 W, the fiber coupling efficiency exceeds 89%, and the external cavity efficiency exceeds 91%. The central wavelength is 852.052 nm (in air), which is tunable from 851.956 nm to 852.152 nm, and the spectral linewidth is 0.167 nm. Research results can be used for cesium alkali metal vapor laser pumping.

Keywords: external cavity feedback; volume Bragg grating; diode laser; beam combining; narrow linewidth; tunable wavelength.

DOI: 10.3788/COL202220.081401

1. Introduction

Diode-laser-pumped alkali metal vapor lasers (DPALs) combine the advantages of solid and gas lasers, such as high quantum efficiency, low thermal effect, and compact structure, and can obtain a high-power laser output while maintaining excellent beam quality. DPALs have been identified as "the preferred solution for megawatt high energy laser"[1–5]. Therefore, DPALs have a wide application prospect in industrial, medical, aerospace, and military fields[6–8].

At present, high-power DPALs are still in the research and development stage due to technologies that must be investigated, such as the homogenization of the gain medium, the cavity structure design, and engineering amplification. Among them, the high-performance pump source is one of the key technical bottlenecks restricting the development of DPALs. For the efficient pumping of alkali metal vapor laser, the diode laser pump source should have the following characteristics. First, the pump source should have high power and power density[9]. Second, the pump source should maintain a narrow spectral linewidth and a stable central wavelength[10]. In terms of power characteristics, the laser power and beam quality should be improved using diode laser beam collimation and beam combination technologies[11–13]. In terms of spectral characteristics, the main problem in using commercial diode lasers as the pump source is the typical spectral linewidth of 2 nm to 5 nm, which is not narrow enough to pump alkali metal vapor lasers. Moreover, the drift of the laser central wavelength with temperature is significant. The alkali metal vapor laser absorption spectrum is very narrow. Consequently, the pump and absorption spectra cannot be strictly matched. Thus, the spectral linewidth must be narrowed while controlling the central wavelength of the diode laser by technical means[14–16].

Over the past years, several research communities have investigated the high-power narrow-linewidth diode laser for DPAL pumping. Li *et al.* reported that a 40 W laser diode array with a linewidth of 0.14 nm and a central wavelength of 780 nm was realized through the external cavity technology of volume Bragg grating (VBG), indicating that the diode laser array can be used for Rb vapor laser pumping[17]. Pandey *et al.* reported on a high-power diode laser pump source for DPALs. This pump is based on a micro-channel water-cooled stack with

collimation in both axes, and the output power is 100 W/bar with a spectral linewidth of 0.06 nm[18]. The conventional external cavity structure includes a fast axis collimation lens, a slow axis collimation lens, and a VBG. However, the VBG has angle selectivity. After the fast and slow axis collimations, the divergence angle of the slow axis still reaches 2°–3° and then affects the external cavity feedback efficiency. In this paper, a combination of a fast axis collimator (FAC), a beam transformation system (BTS), and a slow axis collimator (SAC) as a collimation system is used to shape beam spots and reduce the divergence angles in the fast and slow axes. The divergence angle of the fast and slow axes can be reduced to 0.573°, thereby improving the feedback efficiency of the external cavity.

Starting with DPAL pump source technology, this study investigated diode lasers with high power, high power density, stable spectrum, and narrow linewidth, especially focusing on exploring the efficient external cavity feedback technology based on VBG to improve the external cavity diffraction efficiency[19,20]. A high power of kilowatt (kW) level and a narrow-linewidth laser output are achieved by using conduction-cooled single bars as the unit device and adopting the fast and slow axes beam collimation, beam spatial combination, VBG external cavity feedback, and precision temperature control technologies. The tuning of the central wavelength is also realized by precisely controlling the VBG temperature, laying the foundation for the efficient pumping of DPALs.

2. Experimental Setup

2.1. Research on efficient external cavity feedback technology

In addition to the high output power and power density requirement of the diode laser pump source, the strict matching of the diode laser pump and the alkali metal vapor absorption spectra is critical to obtaining a high-power DPAL output, that is, the central wavelength and the spectral linewidth should be strictly controlled to improve the pumping efficiency and reduce the waste heat generation. According to the principle of energy band transition, the absorption spectrum width of alkali metal atoms is very narrow. Even if the collision broadening effect is generated after filling with high-pressure buffer gas, the absorption spectrum width is only 0.02–0.2 nm. Therefore, the linewidth must be narrowed, and the central wavelength of the diode laser should be stabilized to improve the absorption efficiency of the gain material.

Using VBG for external cavity feedback is a good solution. The diode laser chip with front cavity surface antireflection provides a gain medium and a back cavity surface, and VBG is used as the front cavity surface of the resonant cavity. Under the action of electric excitation, population inversion is realized. The VBG feedback light is used as the seed light, and a laser with a narrow linewidth can be obtained after amplification by a resonator[21]. VBG can realize single-channel adjustment and thus has a low requirement on the consistency of the diode laser unit. The wavelength selection characteristic of VBG makes the diode laser resonant at the diffraction wavelength of the VBG, thereby realizing diode laser wavelength selection and linewidth narrowing. In addition, the diffraction wavelength of VBG varies with the temperature, and the temperature drift coefficient is small. Consequently, the pump laser wavelength can be adjusted by controlling the VBG temperature, and laser wavelength locking and regulation can be realized under precise temperature control.

In this paper, we compare the traditional and new structures through simulations. Compared with the conventional external cavity structure of fast axis collimation, slow axis collimation, and VBG (FAC + SAC + VBG)[22], although the divergence angle of the laser in the fast axis direction can be controlled within the effective feedback angle of the VBG, the minimum slow axis divergence angle after collimation is 2°–3° due to the focal length limitation of the slow axis array collimation lens. The effective feedback's efficiency is further affected by the external cavity fitting error between the laser chip and the VBG, the smile effect of the packaging, and the transmission loss of the VBG. In this study, the conventional external cavity feedback beam shaping structure is optimized, and a new FAC, 45° beam converter, SAC, VBG (FAC + BTS + SAC + VBG) structure is proposed. BTS is used to change the beam direction of the fast and slow axes, which is convenient for beam shaping. Meanwhile, the divergence angle of both the fast and slow axes can be compressed to less than 0.57°. The external cavity feedback structures based on VBG are shown in Figs. 1 and 2.

First, the optical simulation of the FAC + SAC + VBG external cavity feedback structure is carried out. To ensure consistent simulation conditions, we perform the following regulations.

(1) The linear array diode laser is selected as the unit device. The emitter width of the fast and slow axes is 1 μm × 150 μm, and the divergence angle is 60° × 10°.

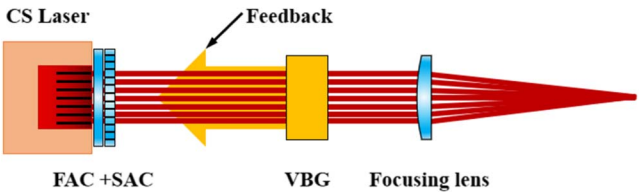

Fig. 1. External cavity feedback structure diagram based on FAC + SAC + VBG.

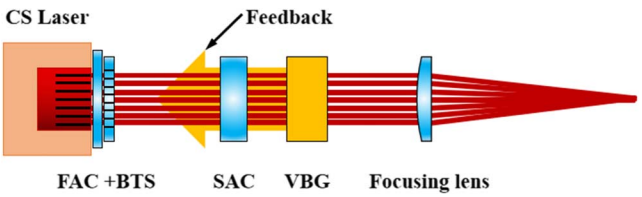

Fig. 2. External cavity feedback structure diagram based on FAC + BTS + SAC + VBG.

The number of emitters of a single bar is 19, and the emitter spacing is 500 μm. Therefore, the filling factor is 30%.

(2) The effective aperture of the VBG is 12 mm × 3.2 mm, and the thickness of the VBG is 3 mm. The external cavity feedback angle is set to 1°, and the diffraction efficiency is set to 100%.
(3) The influence of the optical lens aperture and the coating loss is ignored in the simulation process, and only the aperture filter and acceptance angle of the VBG and the laser chip are considered.
(4) The "smile" effect of the diode laser chip on the optical simulation is ignored.
(5) The linear array diode laser chip can only receive feedback light within the divergence angle of 60° × 10°, and only the feedback light within the 1 μm × 150 μm aperture can be absorbed.
(6) The effective aperture of the VBG is 12 mm × 3.2 mm, and the light beyond this aperture is absorbed. The effective acceptance angle is 1°, and the rest of the light cannot return to the cavity.

FAC and SAC are selected from the lens library of the Zemax software. FAC is the aspheric cylindrical lens with a focal length of 0.3 mm, and SAC is the spherical cylindrical lens array with a focal length of 2.86 mm. The simulation results are shown in Fig. 3.

The simulation results show that the beam size after collimation is 10 mm × 0.4 mm, which is within the effective aperture range of VBG. The divergence angle of the slow axis is approximately 3°, which is three times that of the effective feedback acceptance angle of the VBG. Thus, the external cavity diffraction efficiency of this structure is low.

Figure 4 shows the external cavity diffraction efficiency through aperture filtering and acceptance angle filtering. The overall efficiency is only 32.03%. Therefore, this structure is not conducive to realizing linewidth narrowing through the external cavity feedback.

Second, we simulate the FAC + BTS + SAC + VBG external cavity feedback structure under the same conditions. As shown in Fig. 5, the focal length of the SAC is 12 mm, and the beam size after collimation is 10 mm × 2.4 mm, which is within the effective aperture range of the VBG. The divergence angle of the slow axis is approximately 0.64°, which is near the effective feedback acceptance angle of the VBG.

Figure 6 shows the external cavity diffraction efficiency through aperture filtering and acceptance angle filtering. The overall efficiency of the structure is significantly improved as the divergence angle of the slow axis is effectively controlled, reaching 65.77%.

Finally, we conduct an optical simulation based on the FAC + BTS + SAC + VBG external cavity structure. Increasing the focal length of SAC can theoretically reduce the laser divergence angle and improve the external cavity diffraction efficiency. Thus, the focal length of SAC is set to 15 mm, and the beam size after collimation is 10 mm × 3 mm, which are all within the effective aperture range of the VBG. The divergence angle of the slow axis is approximately 0.48°, as shown in Fig. 7.

As shown in Fig. 8, the external cavity diffraction efficiency is improved to 66.25% when the divergence angle of the slow axis is further reduced. The increase is not obvious, but the vertical beam size is increased by 20%, so the required effective aperture of the VBG is increased. In addition to the external cavity diffraction efficiency of the VBG, the selection of the focal length

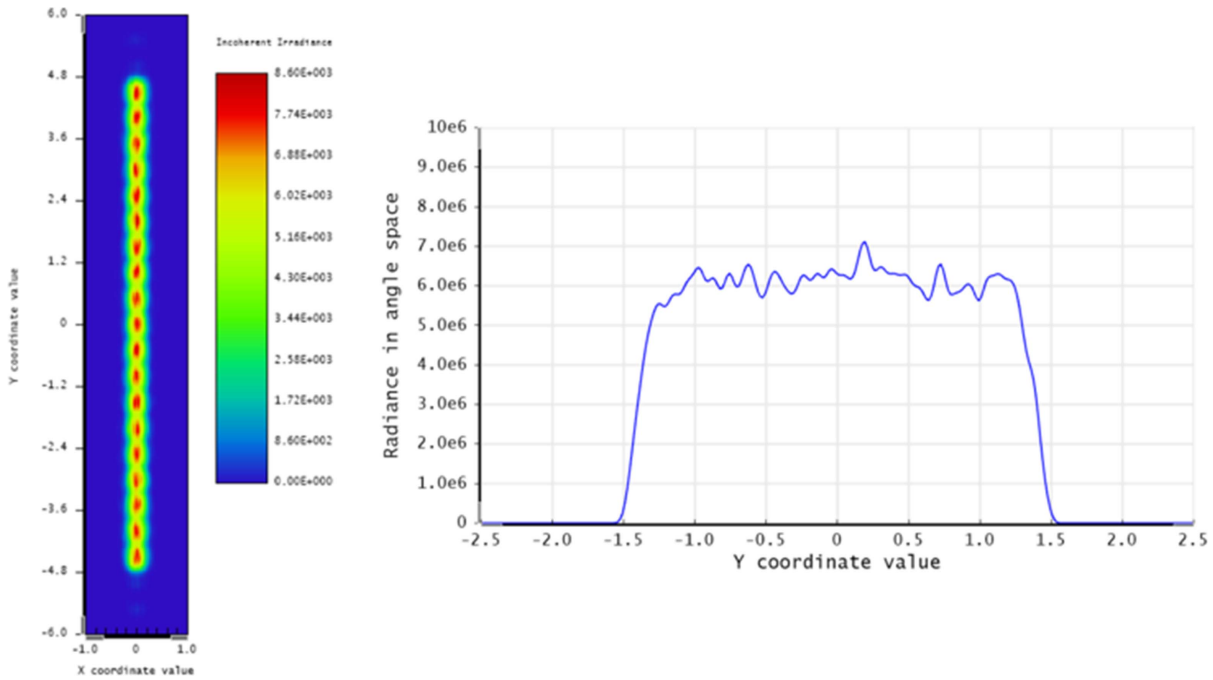

Fig. 3. Beam size and divergence angle after collimation of FAC + SAC + VBG external cavity structure.

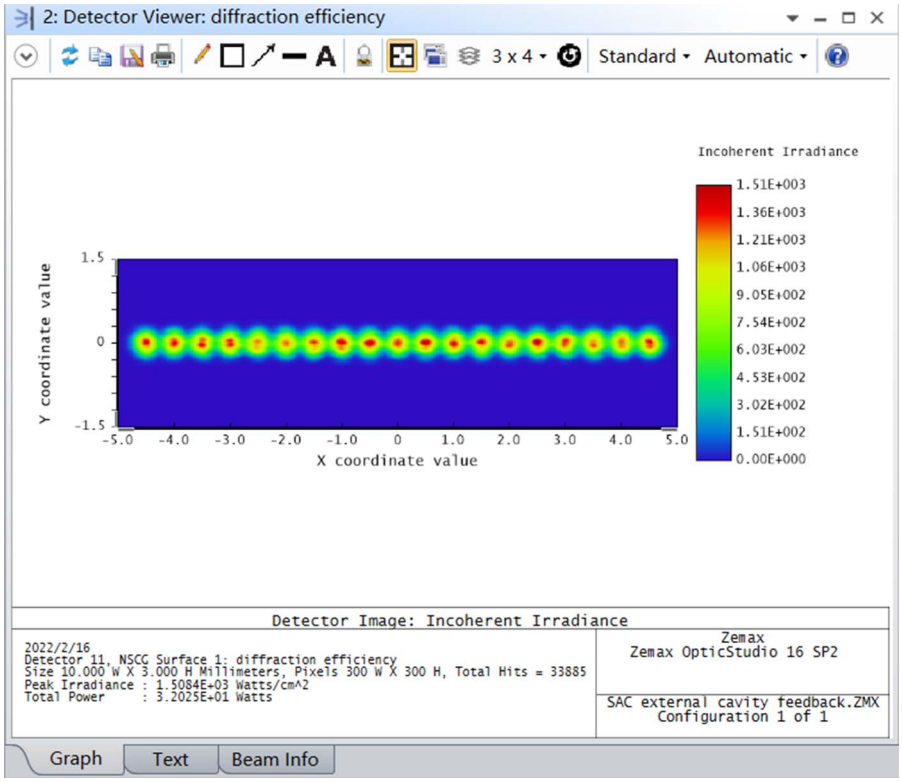

Fig. 4. Effective feedback of FAC + SAC + VBG external cavity structure.

of the SAC should be rationally designed by combining the diode laser beam combination technology.

2.2. Beam shaping structure design

In the external cavity feedback structure based on VBG, to understand the mode competition process between the VBG diffraction efficiency and the facet reflectivity of the laser chip front cavity surface, the approximate formula of spectral locking by VBG can be obtained by using the rate equation[23]:

$$r_3 \geq r_2 \exp\{2\Gamma[g(\lambda_0) - g(\lambda_g)]L\}, \tag{1}$$

where r_3 is the diffraction efficiency of the VBG, r_2 is the facet reflectivity of the laser chip front cavity surface, Γ is the confinement factor of the diode gain region, L is the outer cavity length,

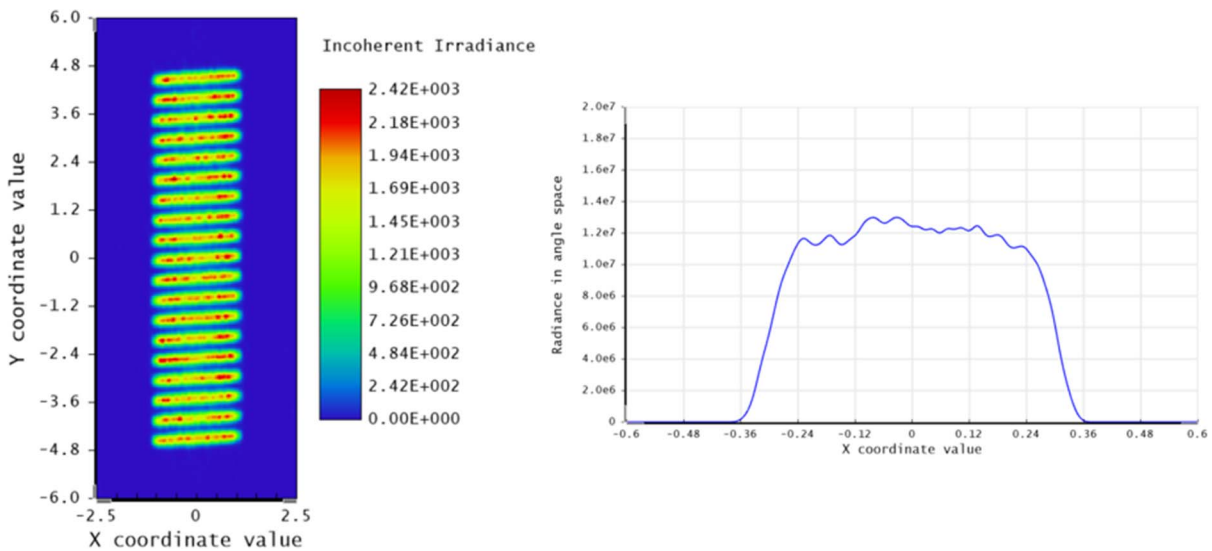

Fig. 5. Beam size and divergence angle after collimation of FAC + BTS + SAC + VBG external cavity structure.

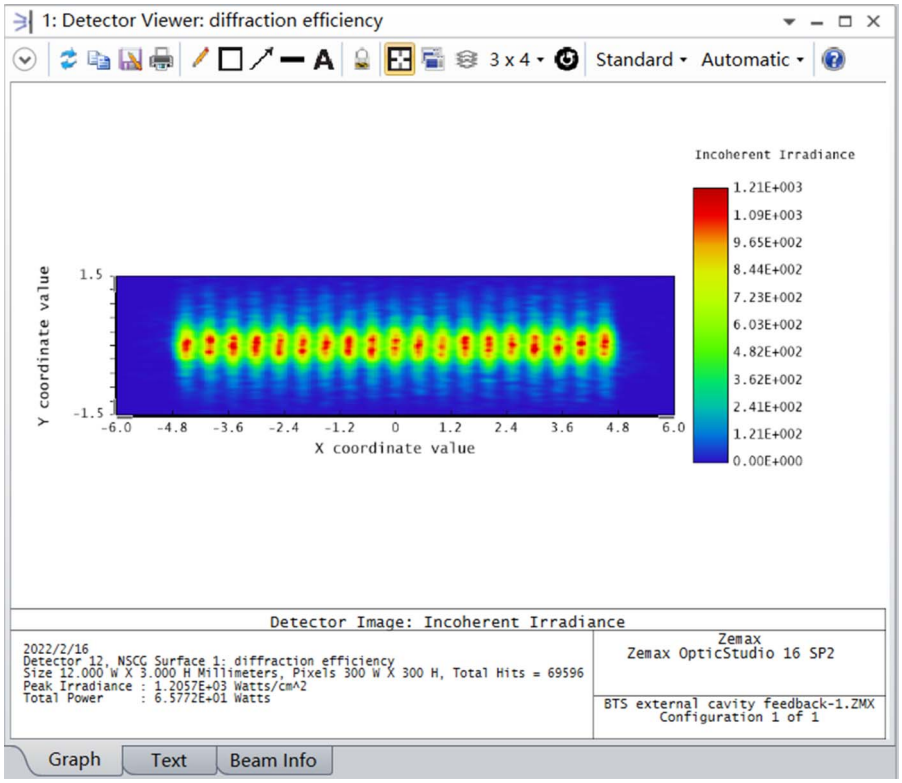

Fig. 6. Effective feedback of FAC + BTS + SAC + VBG external cavity structure.

$g(\lambda)$ is the gain as a function of wavelength, and λ_0 and λ_g are the free running and VBG locking wavelengths, respectively.

From the perspective of spectral locking, to achieve an efficient external cavity feedback and a narrow-linewidth laser output, the reflectivity of the front cavity surface (r_2) of the laser chip must be reduced, and the diffraction efficiency (r_3) of the VBG should be increased. However, for the spectral locking of high-power diode laser chips, the low reflectivity of the front cavity surface will increase the threshold current, and the high antireflection coating will easily cause catastrophic optical mirror damage (COMD). The lower the reflectivity of the front cavity surface is, the more likely it is to be affected by the external cavity feedback, which will improve the optical power density at the local position of the front cavity surface and then accelerate the damage of the front cavity surface. Spectral locking will be difficult when the reflectivity of the front cavity surface is

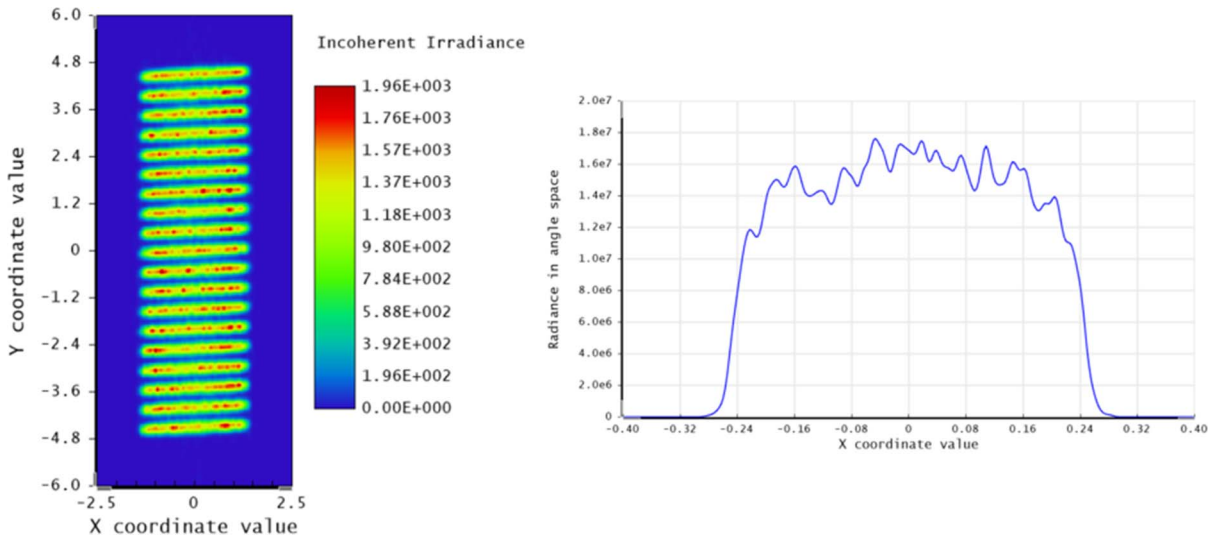

Fig. 7. Beam and divergence angle after collimation of FAC + BTS + SAC + VBG external cavity structure.

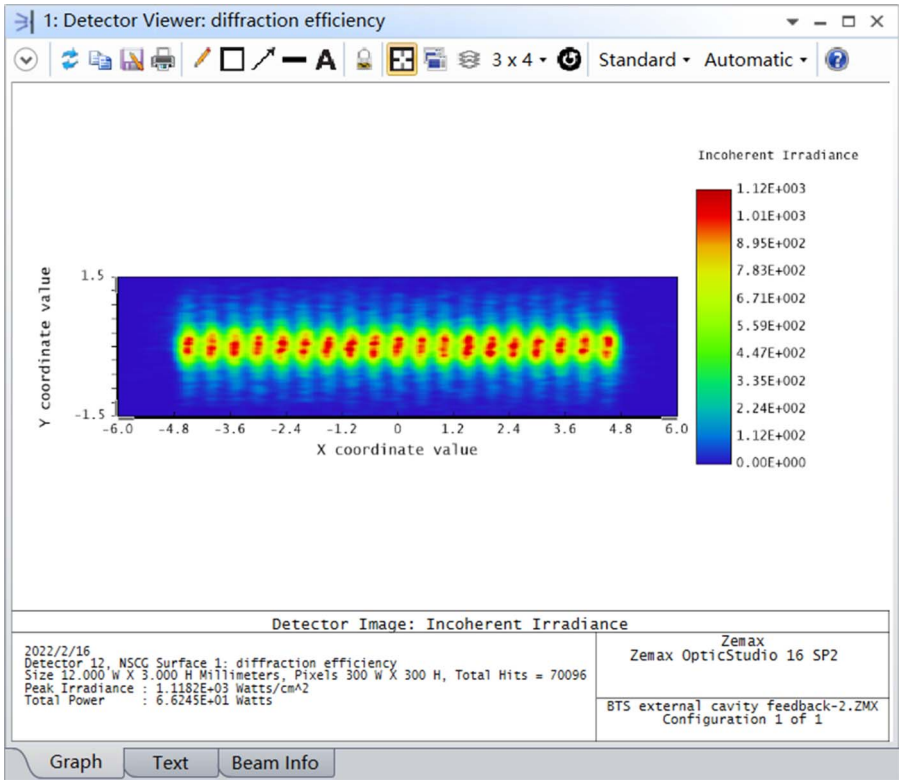

Fig. 8. Effective feedback of FAC + BTS + SAC + VBG external cavity structure.

increased. Thus, the diffraction efficiency of the VBG is inevitably increased. However, the wavelength selective feedback of the VBG will also generate local high-power density in the cavity surface and cause COMD with the increase of the diffraction efficiency. Therefore, the reflectance of the front cavity and the diffraction efficiency of VBG should be reasonably designed and selected to ensure the reliability and spectral locking effect of the laser chip.

Table 1 shows the main parameters of the 852 nm diode laser chip. The central wavelength is 852 ± 2 nm, and the spectral width is less than 3.5 nm. The single bar is composed of 19 emitters, the emitter spacing is 500 μm, and the emitter width of the slow axis is 150 μm. The front cavity surface reflectance coating of the laser chip is 2%–3%, the diffraction efficiency of the VBG is 10% ± 3%, and the diffraction wavelength is 851.7 ± 0.1 nm.

Although the divergence angle in the fast axis direction is large, the beam quality is excellent because the emitter size is small and the beam parameters product (BPP) is near the diffraction limit. However, the BPP in the slow axis direction is very large, so the laser beam must be shaped to reduce the BPP in the slow axis direction. In this study, the BTS beam converter produced by the Limo Company is used, and the focal length is 0.41 mm. The laser beam rotates 90° after passing the BTS, and the divergence angle of the fast axis after collimation is 0.24°, which is simulated by Zemax, as shown in Fig. 9.

In the SAC aspect, the laser beam in the fast and slow axis directions can be exchanged by BTS, requiring no complex SAC array lens for collimation. A single plano-convex cylindrical lens can be used to complete the slow axis direction collimation, and no limit is set for the minimum focal length of an SAC. The divergence angle after collimation is determined by the focal length of the SAC, which is determined by Eq. (2):

Table 1. Typical Parameters of Laser Chip.

Parameters	Unit	Specifications
Center wavelength range	nm	852
Center wavelength tolerance	nm	±2
Spectral width (FWHM)	nm	<3.5
Output power	W	55
Operating current	A	~65
Operating voltage	V	<1.80
Emitter width	μm	150
Number of emitters	/	19
Front cavity surface coating	%	2–3
Vertical far field 95% power in bucket	deg	<60
Lateral far field 95% power in bucket	deg	<10

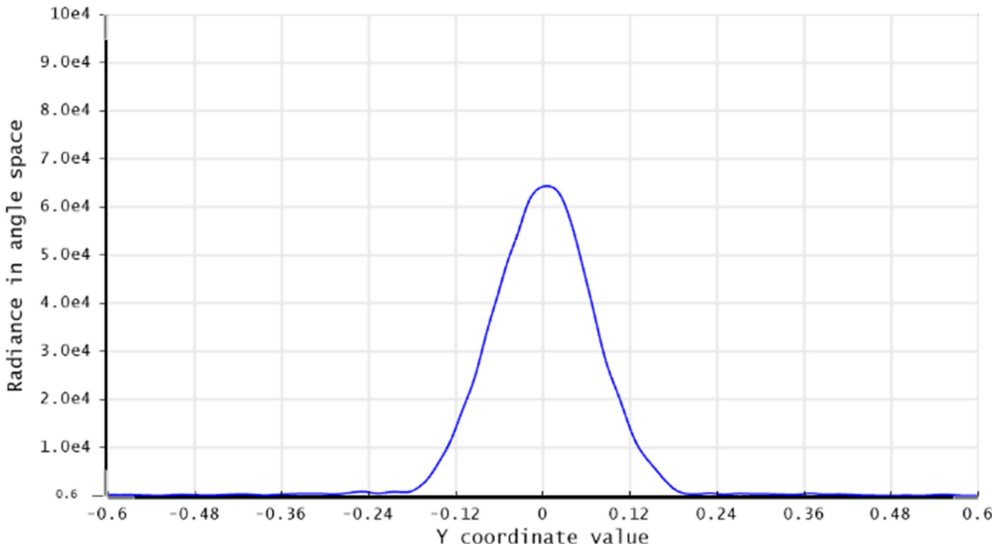

Fig. 9. Simulation results of fast axis divergence angle.

$$f'_{\mathrm{SA}} = \frac{\omega_{\mathrm{SA}}}{2\tan(\theta'_{\mathrm{SA}}/2)}. \tag{2}$$

In the equation, ω_{SA} is the emitter size of the laser chip, f'_{SA} is the focal length of the SAC, and θ'_{SA} is the slow axis divergence angle after collimation. An SAC with a focal length of 15 mm is selected. The calculated beam divergence angle after collimation is approximately 0.57°.

In addition, the beam size after collimation in the slow axis direction must also be considered. Theoretically, the divergence angle can be infinitesimally small, but when the divergence angle decreases, the beam size will increase, which is not conducive to the development of beam combination technology. Thus, the laser divergence angle and beam size should be comprehensively considered. The beam size (ω'_{SA}) in the slow axis direction after collimation is determined by Eq. (3). After calculation, the beam size in the slow axis direction after collimation is approximately 2.36 mm when the slow axis divergence angle before collimation (θ_{SA}) is 10°:

$$\omega'_{\mathrm{SA}} = 2f'_{\mathrm{SA}}\tan(\theta_{\mathrm{SA}}/2). \tag{3}$$

The collimation structure based on FAC, BTS, and SAC is shown in Fig. 10. The divergence angle and beam size in the slow axis direction are detected behind the SAC, and the simulation results are consistent with the theoretical calculation results. The divergence angle in the slow axis is 0.6°, and the beam size is 2.4 mm, as shown in Fig. 11.

To obtain a high-power 852 nm fiber-coupled diode laser with a 1 kW output, the beam combination and fiber coupling technologies should be combined. This scheme uses 24 channels of a single-bar laser with a 55 W output, and the total power is 1320 W. With a beam collimation efficiency of 99%, the beam combination efficiency is 98%, the VBG external cavity feedback efficiency is 90%, and the fiber coupling efficiency is 90%; the 1 kW laser output can be theoretically achieved, thereby satisfying the design requirements.

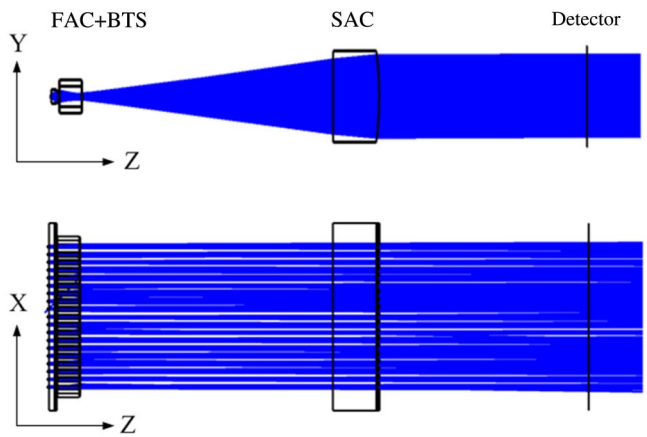

Fig. 10. Simulation diagram based on FAC + BTS + SAC collimation structure.

The height of the mechanical ladder based on the modular distributed structure is designed using space beam combination technology. As shown in Fig. 12, two laser paths are designed in the *X* direction, and the size of the laser beam of each path is approximately 10 mm, so the total beam size of the two laser paths after spatial combination in the *X* direction is 20 mm. Twelve lasers are placed along the steps in the *Y* direction, and the size of the single laser beam in this direction is 2.4 mm, so the total beam size of the 12 lasers in the *Y* direction is 28.8 mm. Considering that the mechanical ladder distribution structure has a tendency to block part of the laser beam, the distance between the two laser beams in the *X* direction increases by 2 mm, and the total length is 22 mm. The step height in the *Y* direction is designed as 2.5 mm, so the beam size in the *X* direction is 30 mm.

In this scheme, an aspheric lens with a diameter of 50 mm and a focal length of 100 mm is used as the focusing lens. The core

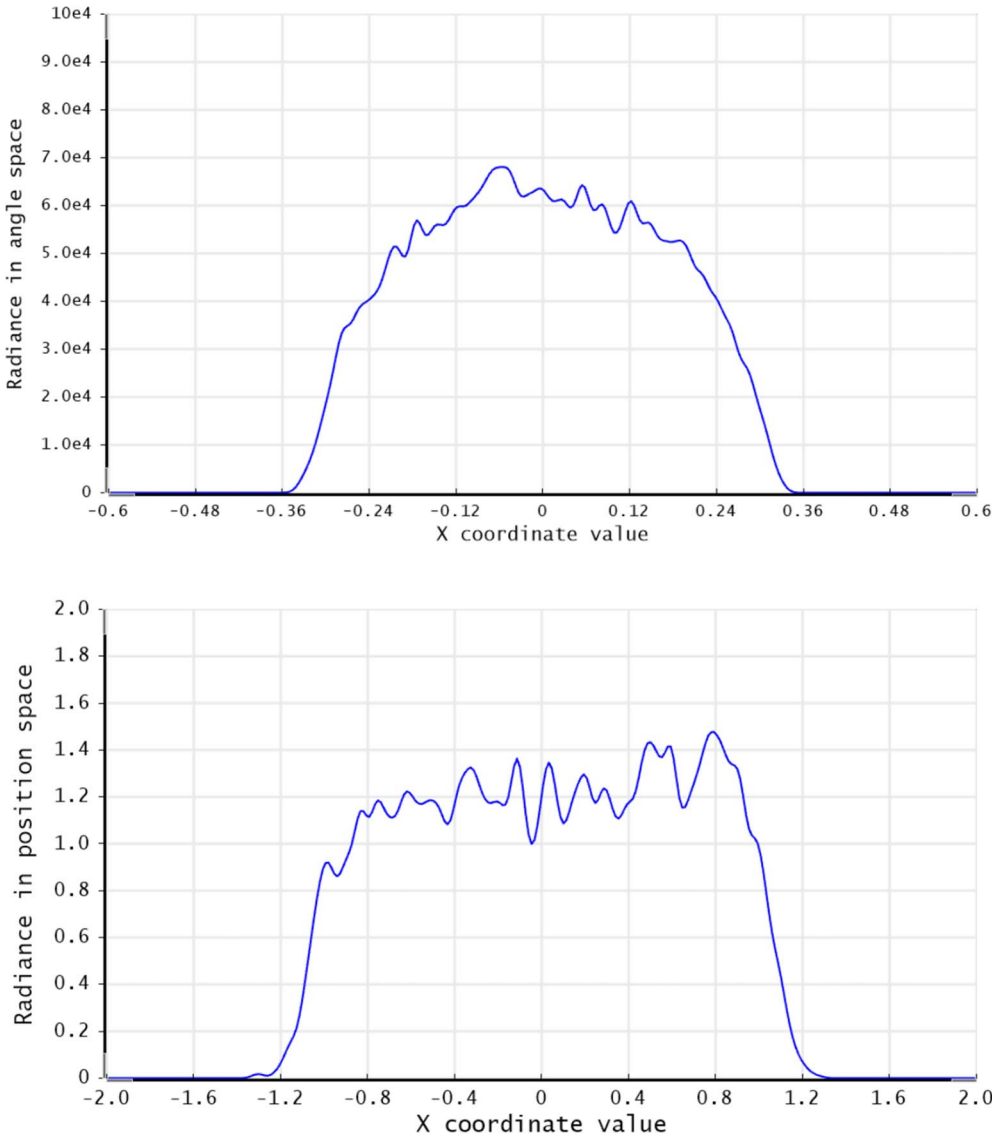

Fig. 11. Simulation results of slow axis divergence angle and beam size.

diameter of the optical fiber is 1000 μm, and the numerical aperture is 0.22. When the initial power is 1320 W, the output power from the optical fiber is 1282 W, so the fiber coupling efficiency is approximately 97.1%. Figure 13 shows the simulated laser beam from the optical fiber.

3. Results and Discussions

In the experiment, the power of the free running laser, beam shaping, VBG external cavity feedback, and fiber coupling are tested. The experimental results are shown in Fig. 14. When the water-cooling temperature is 20°C and the operating current is 65 A, the total output power of the 24-channel laser measured by an Ophir power meter is 1315 W. After the collimation and space beam combination based on FAC, BTS, and SAC, the test power is 1244 W under the same conditions, and the optical–optical conversion efficiency is 94.6%. VBG is added to the optical system for external cavity feedback; after wavelength locking and temperature control, the total output power is 1136 W, and the external cavity feedback efficiency is 91.3%. Finally, the combined beam is coupled into the fiber through the focusing lens. The experiment results show that at 65 A, the power from the fiber is 1013 W, the fiber coupling efficiency is 89.17%, and the total electric–optical conversion efficiency is 42.17% under the same conditions. Figure 15 shows a picture of the laser.

As shown in Fig. 16, an Ando AQ6317B fiber optic spectrometer is used for spectral measurement. Under 65 A of operating current, the VBG temperature is separately controlled by controllers according to different VBG temperatures and manufacturing tolerances. A central wavelength of 852.052 nm (in air) and a spectral width of 0.167 nm (FWHM) are achieved when the temperature of the 24 channels is within 35°C ± 5°C.

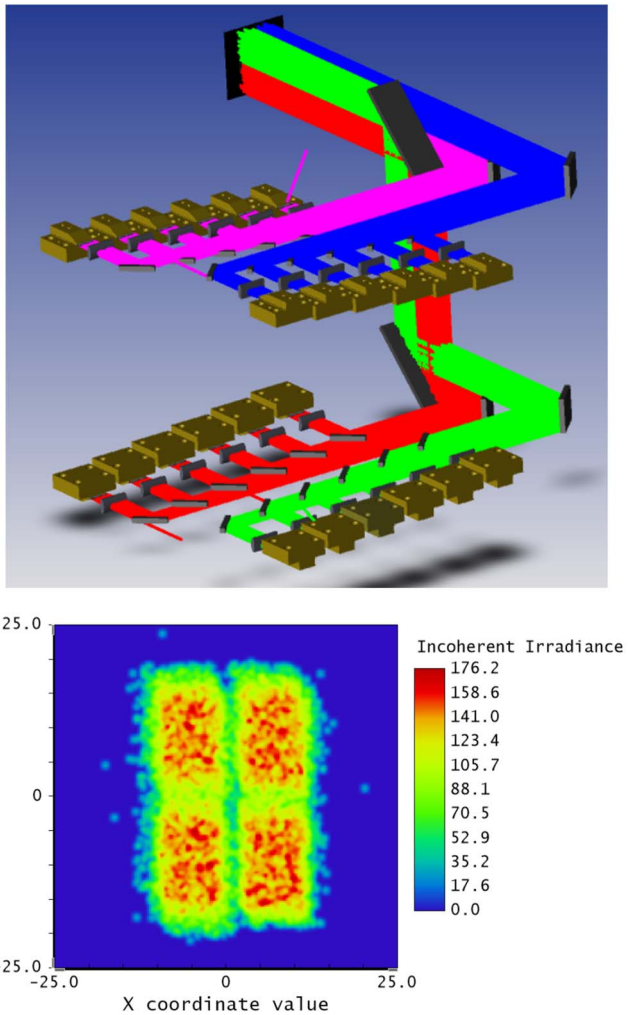

Fig. 12. Simulation diagram of laser beam combination.

As shown in Fig. 17, the tuning of the central wavelength is realized by adjusting the VBG temperature. When the temperature of the 24 channels is within 25°C ± 5°C, a central wavelength of 851.956 nm (in air) and a spectral width of 0.166 nm (FWHM) are achieved. When the temperature of

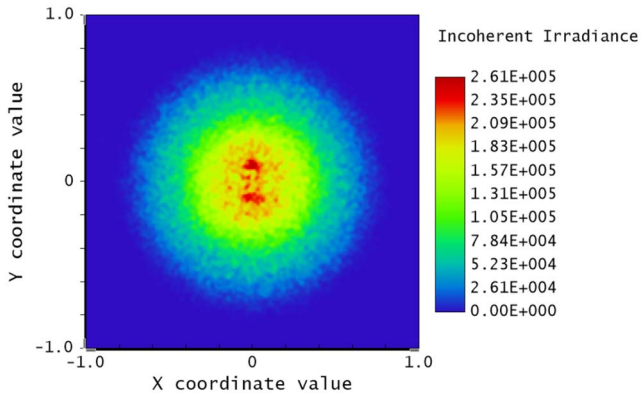

Fig. 13. Beam spot after optical fiber.

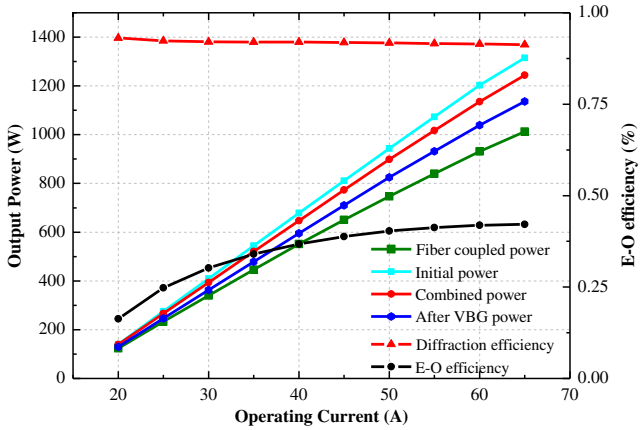

Fig. 14. Power–current–efficiency curve.

Fig. 15. Photograph of an 852 nm kW class narrow-linewidth laser.

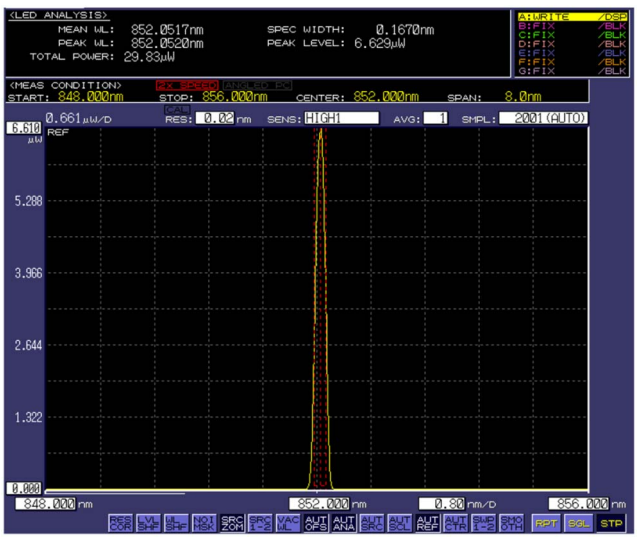

Fig. 16. Laser spectrum at 35°C ± 5°C temperature control.

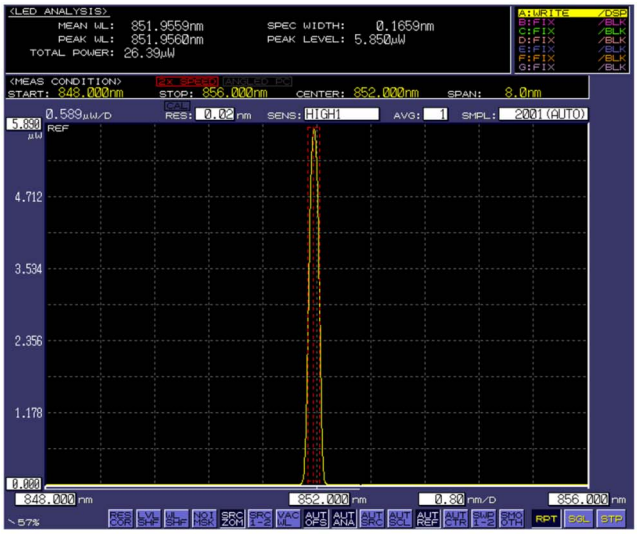

(a)

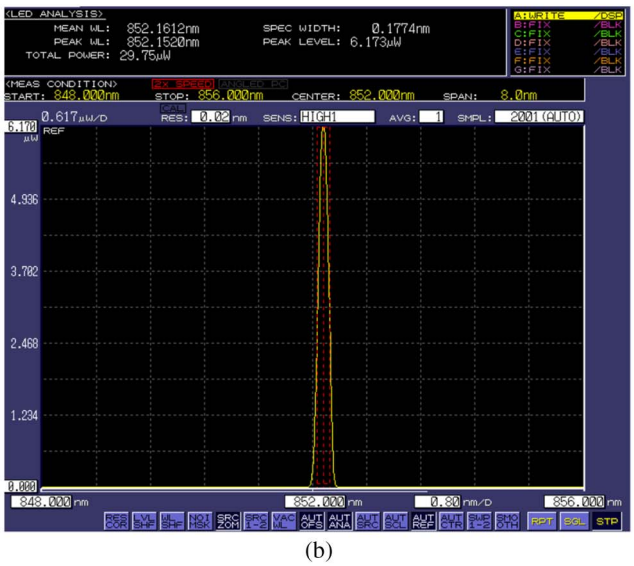

(b)

Fig. 17. Laser spectrum at (a) 25°C ± 5°C and (b) 50°C ± 5°C temperature control.

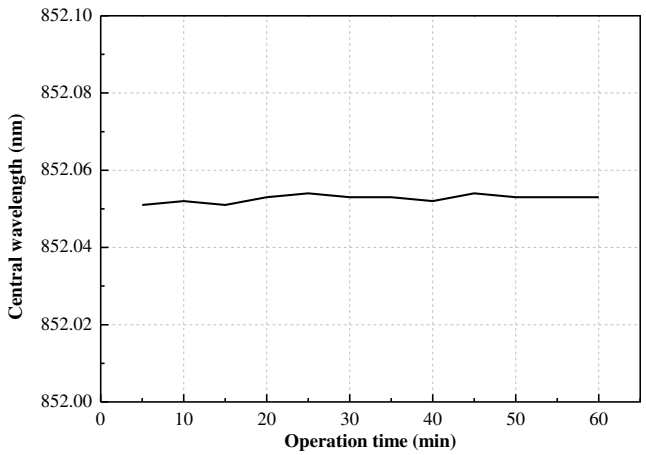

Fig. 18. Variation of central wavelength with operation time.

the 24 channels is in the range of 50°C ± 5°C, the central wavelength is 852.152 nm (in air), and the spectral width is 0.177 nm (FWHM), so the temperature drift coefficient is approximately 0.0078 nm/°C.

As described above, for the efficient pumping of alkali metal vapor lasers, diode lasers should have high-power output and stable spectral characteristics. The central wavelength and spectral linewidth cannot have a large shift, especially when working for a long time. In this paper, the spectral stability of the external cavity feedback diode laser is tested experimentally. Under an operating current of 65 A and a controlling temperature of 35°C ± 5°C, the spectral characteristics are measured for 1 h of operation time. The results are shown in Figs. 18 and 19. The central wavelength shifts from 852.051 nm to 852.054 nm, and the spectrum linewidth fluctuates from 0.166 nm to 0.168 nm. The experimental results show that the laser has a good spectral stability and can meet the needs of high-efficiency pumping DPALs over a long operation time.

Figure 20 shows three energy levels of cesium (Cs) atoms. The electrons will be excited from the ground $6^2S_{1/2}$ level to the $6^2P_{3/2}$ level under the 852.35 nm vacuum wavelength of the pumping laser, which can be collisionally broadened by adding a buffer gas, such as helium. Then, the electrons will relax from

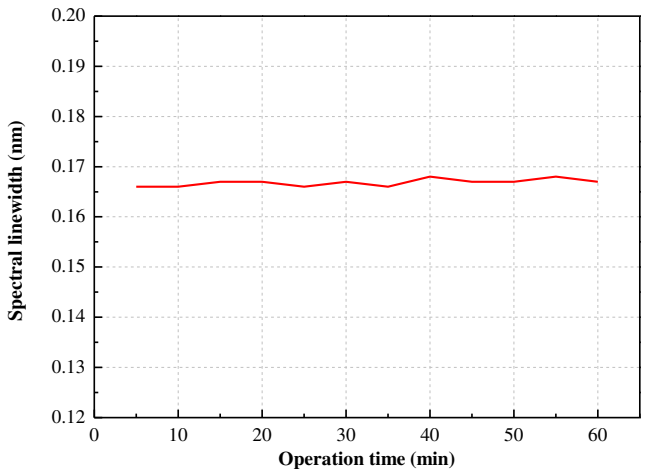

Fig. 19. Variation of spectral linewidth with operation time.

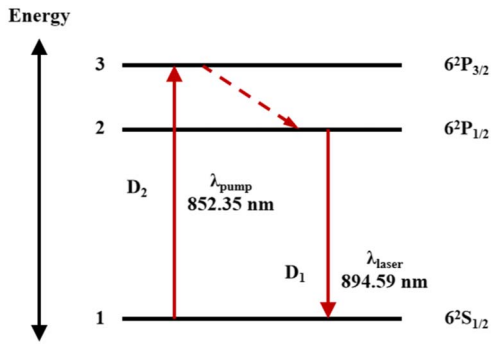

Fig. 20. Diagram of energy levels of cesium atoms.

the $6^2P_{3/2}$ level to the $6^2P_{1/2}$ level. When the pump intensity reaches the threshold value, population inversion can be achieved, and the laser with an 894.59 nm wavelength will be produced[24].

For high-efficiency Cs metal vapor laser pumping, through theoretical research and experimental design, a high-power and narrow-linewidth diode laser pump source with an output power more than 1 kW and a linewidth less than 0.2 nm is realized. By controlling the temperature of the VBG, the central wavelength can be adjusted from 851.956 nm to 852.152 nm in air. The spectrum of the diode laser can strictly match the absorption spectrum of the Cs metal vapor laser. When the buffer gas with different concentrations or pressures is filling the gain cells, the matching of the pump and absorption spectra can be realized by adjusting the VBG temperature. Therefore, the high-power narrow-linewidth diode laser pump source has a broad application prospect.

4. Conclusions

In this paper, the FAC + BTS + SAC + VBG structure is proposed to compress the divergence angle of the laser incident on the VBG. The simulation results show that the proposed scheme can improve the external cavity feedback efficiency compared with the traditional structure. By combining the diode laser beam collimation, space beam combination, external cavity feedback, and fiber coupling technologies, a high-power and narrow-linewidth diode laser with a central wavelength of 852.052 nm (in air), a spectral width of 0.167 nm, and an output power of 1013 W is developed, and the tuning of the central wavelength is realized by controlling the temperature of the VBG. The research results can be applied to the efficient pumping of a Cs metal vapor laser.

Acknowledgement

This work was supported by the National Natural Science Foundation of China (NSFC) (No. 61991433), Pilot Project of CAS (No. XDB43030302), Equipment Pre-research (No. 2006ZYGG0304), Key Research and Development Project of Guangdong Province (No. 2020B090922003), and R&D Program of Jilin Province (No. 20190302042GX).

References

1. B. V. Zhdanov and R. J. Knize, "Diode pumped alkali lasers," Proc. SPIE **8187**, 818707 (2011).
2. I. Auslender, E. Yacoby, B. D. Barmashenko, and S. Rosenwaks, "General model of DPAL output power and beam quality dependence on pump beam parameters: experimental and theoretical studies," J. Opt. Soc. Am. B **35**, 3134 (2018).
3. R. Luzon, S. Kostyukovets, I. Auslender, N. Mayorkas, E. Yacoby, B. D. Barmashenko, and S. Rosemwaks, "Improving the beam quality of DPALs by refractive index gradients induced by the pump beam in the heated gain medium: experimental verification of the theoretical prediction," J. Opt. Soc. Am. B **38**, 550 (2021).
4. C. Xia, J. Huang, C. Su, X. Xu, and B. Pan, "Theoretical research of time dependent pulsed diode-pumped Rb vapor laser," Opt. Laser Technol. **133**, 106529 (2021).
5. S. Wang, J. Han, G. An, W. Zhang, H. Cai, Q. Yu, X. Liu, K. Dai, A. Alghazi, and Y. Wang, "Demonstration of a dual-wavelength alkali laser with a mixed rubidium–cesium vapor cell," Opt. Commun. **458**, 124728 (2020).
6. F. Gao, F. Chenuo, and L. H. Guo, "Review on diode-pumped alkali vapor laser," Optik **124**, 4353 (2013).
7. Q. Zhu, B. Pan, L. Chen, Y. Wang, and X. Zhang, "Analysis of temperature distributions in diode-pumped alkali vapor lasers," Opt. Commun. **283**, 2406 (2010).
8. Y. J. Wang, B. L. Pan, Q. Zhu, and J. Yang, "A kinetic model for diode pumped rubidium vapor laser," Opt. Commun. **284**, 4045 (2011).
9. T. Koenning, D. Irwin, D. Stapleton, R. Pandey, T. Guiney, and S. Patterson, "Narrow line diode laser stacks for DPAL pumping," Proc. SPIE **8962**, 89620F (2014).
10. Z. N. Yang, H. Y. Wang, Q. S. Lu, W. H. Hua, and X. J. Xu, "An 80-W laser diode array with 0.1 nm linewidth for rubidium vapor laser pumping," Chin. Phys. Lett. **28**, 104202 (2011).
11. M. Werner, C. Wessling, S. Hengesbach, M. Traub, and H. D. Hoffmann, "100 W/100 μm passively cooled, fiber coupled diode laser at 976 nm based on multiple 100 μm single emitters," Proc. SPIE **7198**, 71980P (2009).
12. J. Malchus, V. Krausea, A. Koestersa, and D. G. Matthews, "A 25 kW fiber-coupled diode laser for pumping applications," Proc. SPIE **8965**, 89650B (2014).
13. T. Könning, F. Harth, P. König, P. Wolf, M. Stoiber, H. Kissel, and B. Köhler, "Kilowatt-class high power diode lasers at 450 nm," Proc. SPIE **11262**, 112620N (2020).
14. D. Pabœuf, D. Vijayakumar, O. B. Jensen, B. Thestrup, J. Lim, S. Sujecki, E. Larkins, G. Lucas-Leclin, and P. Georges, "Volume Bragg grating external cavities for the passive phase locking of high-brightness diode laser arrays: theoretical and experimental study," J. Opt. Soc. Am. B **28**, 1289 (2011).
15. G. J. Steckman and F. Havermeyer, "High spatial resolution measurement of volume holographic gratings," Proc. SPIE **6136**, 613602 (2006).
16. C. Schnitzler, S. Hambuecker, O. Ruebenach, V. Sinhoff, G. Steckman, L. West, C. Wessling, and D. Hoffmann, "Wavelength stabilization of HPDL array–fast-axis collimation optic with integrated VHG," Proc. SPIE **6456**, 645612 (2007).
17. Z. Li, R. Tan, C. Xu, and L. Li, "Laser diode array with narrow linewidth for rubidium vapor laser pumping," High Power Laser Part. Beams **25**, 875 (2013).
18. R. Pandey, D. Merchena, D. Stapletona, D. Irwina, C. Humblea, and S. Patterson, "Narrow-line, tunable, high-power, diode laser pump for DPAL applications," Proc. SPIE **8733**, 873307 (2013).
19. L. S. Meng, B. Nizamov, P. Madasamy, J. K. Brasseur, T. Henshaw, and D. K. Neumann, "High power 7-GHz bandwidth external-cavity diode laser array and its use in optically pumping singlet delta oxygen," Opt. Express **14**, 10469 (2006).
20. P. Leisher, K. Price, S. Karlsen, D. Balsley, D. Newman, R. Martinsen, and S. Patterson, "High-performance wavelength-locked diode lasers," Proc. SPIE **7189**, 719812 (2009).
21. G. J. Steckman, W. Liu, R. Platz, D. Schroeder, C. Moser, and F. Havermeyer, "Volume holographic grating wavelength stabilized laser diodes," IEEE J. Sel. Top. Quantum Electron. **13**, 672 (2007).
22. R. McBride, N. Trela, J. J. Wendland, and H. J. Baker, "Extending the locking range of VHG-stabilized diode laser bars using wavefront compensator phaseplates," Proc. SPIE **8039**, 80390F (2011).
23. Y. Li, V. Negoita, T. Barnowski, S. Strohmaier, and G. Treusch, "Wavelength locking of high-power diode laser bars by volume Bragg gratings," in *IEEE Photonics Society Summer Topical Meeting Series* (IEEE, 2012), p. 29.
24. W. F. Frupke, "Diode pumped alkali lasers (DPALs)-a review (revl)," Prog. Quantum Electron. **36**, 4 (2012).